

# Communication

## Compact Dual-Polarized Cross-Slot Antenna With Colocated Feeding

Xu Qin and Yue Li 

**Abstract**—In this communication, a dual-polarized cross-slot antenna is proposed with a relative small dimension. Orthogonal polarizations with high port isolation are provided by the cross-slot structure. A dual-mode colocated feeding network is properly integrated with the cross slot, without occupying extra area. Therefore, the overall dimension of the proposed antenna is only  $0.293\lambda_0 \times 0.293\lambda_0 \times 0.008\lambda_0$  ( $\lambda_0$  is the free space wavelength at center frequency). A prototype is fabricated and measured to prove the design strategy. In such a compact antenna volume, the  $-10$  dB impedance bandwidths for both orthogonal polarizations are over 6%, with the port isolation better than 30 dB and radiation efficiency over 68%, exhibiting potential applications in space-limited systems, such as access points and portable base stations.

**Index Terms**—Antenna diversity, antenna feed, compact dimension, cross slot, dual polarized antenna.

### I. INTRODUCTION

With the rapid development of wireless communications, the dual-polarization antenna is now widely applied in multiple-input multiple-output (MIMO) and diversity systems with the merit of high spectrum efficiency. Compact antenna dimension is usually required in small base stations and portable devices. Therefore, designing a dual-polarized antenna with both small dimension and high port isolation is attractive but challenging.

Different kinds of dual-polarized antennas have been introduced and validated in recent literatures. Cross dipoles [1]–[7], microstrip antennas [8]–[13], and slot antennas [14]–[21] have been widely used in dual-polarized antenna design. Cross dipoles usually have simple structure, and microstrip antennas are adopted for their low profile, while bidirectional radiation is usually achieved in slot antennas. To increase the isolation between ports, several methods have been presented. Antennas in [5]–[7] use differentially fed dipoles to realize high isolation. Properly designed feeding structures, such as air bridge [22]–[24] and aperture coupling [25], [26], are adopted to achieve a satisfying isolation better than 30 dB. Generally, the isolation between two ports decreases as the size of the antenna shrinks. Antennas in [27] and [28] achieved a relatively small volume, but the isolation is approximately 21.3 dB [27] and 23 dB [28]. Slot antennas are feasible solutions in compacting dimensions while maintaining high isolation. Rectangle slot [14]–[16], triangle slot [17], and circle slot [18] perform satisfactorily in realizing two orthogonal polarizations with high port isolation. Cross slots also depict acceptable characteristics in [19]–[21]. In those designs, the feeding structure occupies extra space, increasing the overall area of the antenna.

Manuscript received April 19, 2019; revised June 19, 2019; accepted July 20, 2019. Date of publication August 27, 2019; date of current version October 29, 2019. This work was supported in part by the National Natural Science Foundation of China under Grant 61771280, in part by the Natural Science Foundation of Beijing Manipulate under Contract 4182029, and in part by the Tsinghua University Initiative Scientific Research Program under Contract 2019Z08QCX16. (Corresponding author: Yue Li.)

The authors are with the Department of Electronic Engineering, Tsinghua University, Beijing 100084, China, and also with the Beijing National Research Center for Information Science and Technology, Tsinghua University, Beijing 100084, China (e-mail: lyee@tsinghua.edu.cn).

Color versions of one or more of the figures in this communication are available online at <http://ieeexplore.ieee.org>.

Digital Object Identifier 10.1109/TAP.2019.2936758

0018-926X © 2019 IEEE. Personal use is permitted, but republication/redistribution requires IEEE permission. See [http://www.ieee.org/publications\\_standards/publications/rights/index.html](http://www.ieee.org/publications_standards/publications/rights/index.html) for more information.

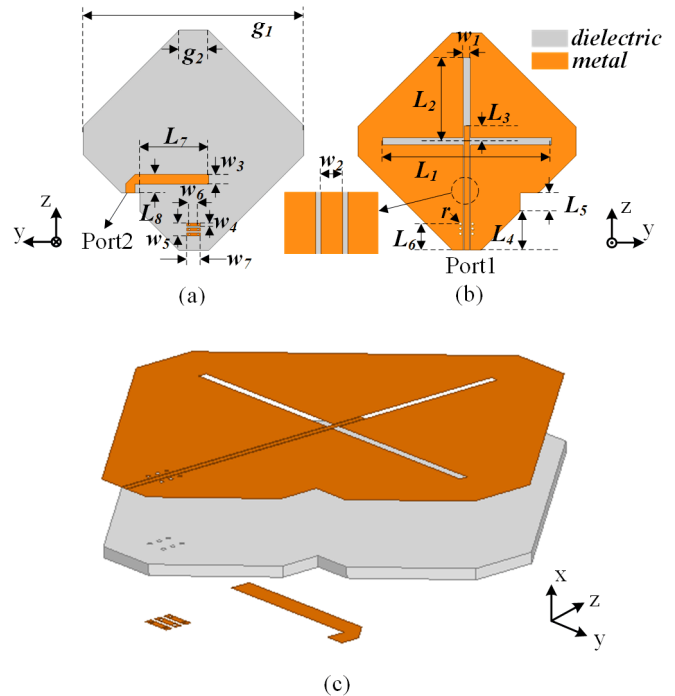


Fig. 1. Geometry and dimensions of the proposed antenna. (a) Back, (b) front, and (c) perspective views.

In this communication, a compact dual-polarized cross-slot antenna is proposed. The antenna is based on a single layer of substrate, and employs a simple colocated feeding structure. The cross slot, as the main radiating aperture, provides two orthogonal polarizations. The antenna is excited by the coplanar waveguide (CPW) colocated with the slot. Therefore, the feeding structure occupies no extra space in this design, and the overall dimensions of the antenna are reduced. By integrating the feeding network and radiating aperture, the size of the antenna is compacted to  $0.293\lambda_0 \times 0.293\lambda_0 \times 0.008\lambda_0$ , with a high port isolation of 30 dB.

### II. ANTENNA DESIGN

Fig. 1 presents the general structure of the proposed dual-polarized cross-slot antenna excited by the colocated CPW feeding network. The antenna is fabricated on a FR4 substrate with a relative permittivity of 4.0 and loss tangent of 0.02. The thickness of the substrate is 1 mm. Fig. 1(a) shows the structure of the L-shaped microstrip line on the back side of the substrate. The metal on the front side serves as the ground plane of the microstrip line. A small portion of the substrate is cut for the convenience of soldering the connectors to excite the microstrip line. As plotted in Fig. 1(b), the cross slot is positioned on the front side of the substrate to operate as the radiating aperture. The CPW is colocated with the vertical slot. The orthogonal slots are with the same dimensions of  $w_1 \times L_1$ , supporting the horizontal

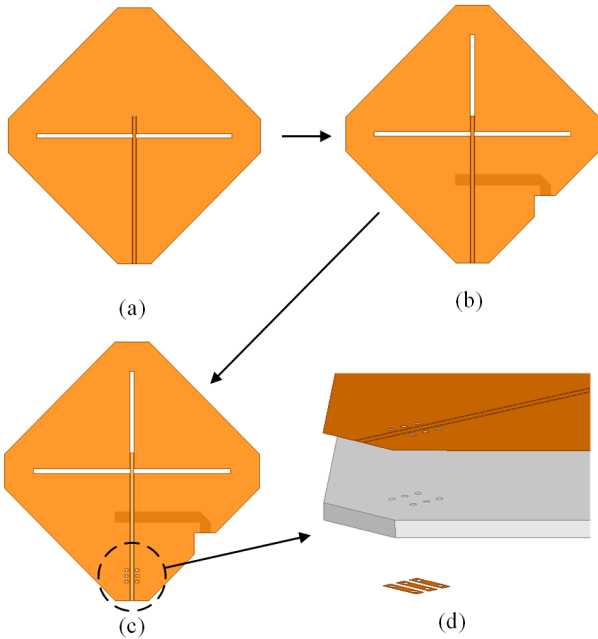


Fig. 2. (a)–(c) Evolution of the proposed dual-polarized antenna. (d) Perspective view of the air bridge.

and vertical polarizations, respectively. In this way, dual polarizations are achieved within single layer of substrate without occupying extra area to arrange the CPW feeding.

It is known that there are orthogonal modes supported in CPW [14]. The mode with symmetric electric field distribution is noted as the even mode, while the odd mode has asymmetric electric field distribution. The two modes have orthogonal electric field distributions with high isolation. Fig. 2 illustrates the design evolution of the proposed dual-polarized antenna fed by the collocated CPW feeding structure. First, in Fig. 2(a), the single horizontal slot is excited by the CPW. The CPW operates at its normal even mode, and transmits energy to the horizontal slot to excite the vertical polarization. Then, as shown in Fig. 2(b), the vertical slot is adopted to support the horizontal polarization. The microstrip line on the back side couples the energy to the CPW and excites the odd mode, which excites the horizontal polarization in the vertical slot. The field distributions of vertical polarization and horizontal polarization are depicted in Fig. 3(a) and (b). The odd mode in the CPW is with an identical electric field distribution similar to the one inside the vertical slot, and the inner conductor of the CPW is an equipotential body that has no influence on the slot mode. Therefore, the CPW also serves as a portion of radiating aperture supporting the horizontal polarization. Because of the orthogonality of the dual modes inside the CPW, the two polarizations are with high isolation. As shown in Fig. 3(c) and (d), the two polarizations excited by orthogonal modes of the CPW also have orthogonal electric field distributions in the CPW, and therefore, have little influence on each other. Finally, air bridges are introduced in Fig. 2(c). Due to the presence of CPW, the vertical slot has an open end at the bottom. For this reason, the air bridges connecting the outer conductor of the CPW are utilized to “close” the vertical slot, as shown in Fig. 2(d). When CPW is at the even mode, the air bridges are with no influence because the outer conductor on both side of the CPW has the same electric potential. When the odd mode of the CPW is excited, the air bridges can provide shorting boundary for the vertical slot. As mentioned above, the CPW is used as the feeding structure of the dual polarizations and the radiating aperture

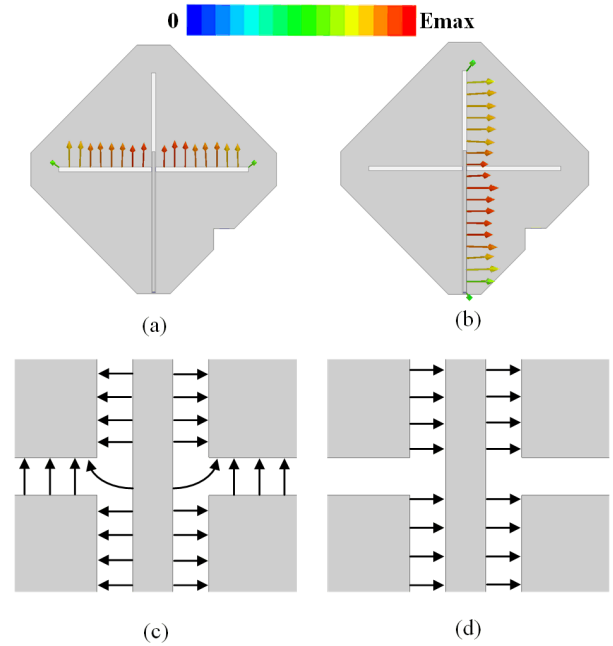


Fig. 3. Vector electric field distributions of the two orthogonal polarizations. (a) Vertical polarization in the slot. (b) Horizontal polarization in the slot. (c) Vertical polarization in the CPW. (d) Horizontal polarization in the CPW.

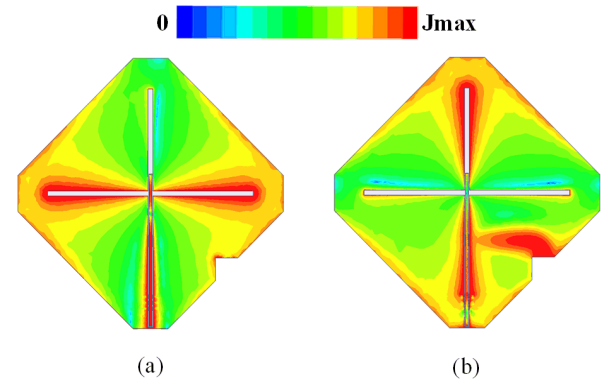


Fig. 4. Current distributions of the two polarizations at 2.5 GHz, excited by (a) Port1. (b) Port2.

simultaneously. By adopting the collocated CPW feeding structure, the antenna can be integrated in a compact area.

The proposed design is optimized using the finite element method solver of Ansoft high-frequency structure simulator (HFSS). The length of the horizontal slot  $L_1$  determines the resonant frequency of the vertical polarization, while  $L_2$  and the position of the air bridges determine the resonant frequency of the horizontal polarization. By adjusting the position of the air bridges, the two slots have the same length and work in the same frequency. It is seen in Fig. 4 that the cross slot is working with the orthogonal polarizations at 2.5 GHz. The microstrip line on the back side and the CPW on the front side have characteristic impedance of  $50 \Omega$ . The parameters  $L_7$  and  $L_8$  are tuned for impedance matching of Port2, and the length of  $L_3$  has significant impact on the matching performance of Port1, as shown in Fig. 5. Detailed parameters are listed in Table I.

### III. EXPERIMENTAL RESULTS

A prototype of the proposed antenna was fabricated by the standard printed circuits board (PCB) technique. And the prototype is also

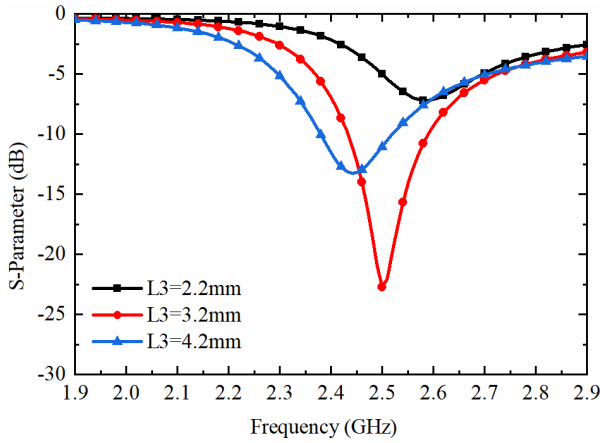


Fig. 5. Simulated  $S_{11}$  with different values of  $L_3$ .

TABLE I  
DETAILED DIMENSIONS (UNIT: mm)

$g_1$	$g_2$	$w_1$	$w_2$	$w_3$	$w_4$	$w_5$	$w_6$	$w_7$
45	6	0.8	0.54	1.9	0.6	2.6	1.8	2.8
$L_1$	$L_2$	$L_3$	$L_4$	$L_5$	$L_6$	$L_7$	$L_8$	$r$
34.8	17.4	3.2	8	3.8	5.3	14	3.7	0.2

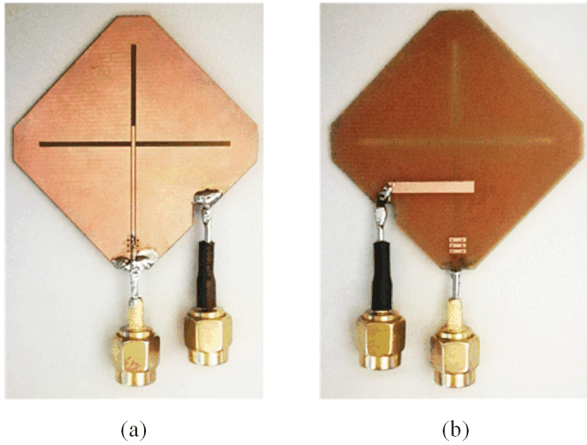


Fig. 6. (a) Front and (b) back views of the fabricated prototype.

measured to verify the design based on the optimized dimensions in Table I. Fig. 6 shows the front and the back views of the prototype. Two 50  $\Omega$  coaxial cables were used to excite the proposed dual-polarized antenna. The S-parameters and the radiation patterns were measured by a vector network analyzer (Agilent E5071B) and the far-field anechoic chamber (ETS-LindgrenAMS8500), respectively. Fig. 7 shows the simulated and measured S-parameters of the prototype, the measured and simulated results agree with each other fairly well. The simulated  $-10$  dB impedance bandwidths are 2.44–2.60 GHz for Port1 and 2.44–2.59 GHz for Port2. While in the experiment, the measured  $-10$  dB impedance bandwidths are 2.44–2.59 GHz for Port1 and 2.44–2.60 GHz [bad break] for Port2. The simulated isolation between the two feeding ports is better than 27 dB, and the measured result is better than 30 dB. The slight difference between the simulated and measured results could come from

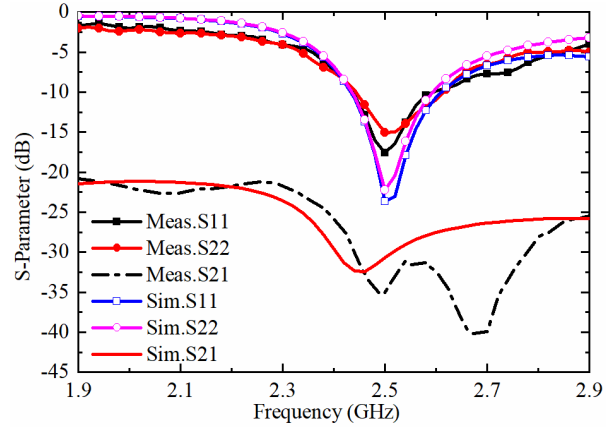


Fig. 7. Simulated and measured S-parameters of the proposed dual-polarized antenna and the fabricated prototype.

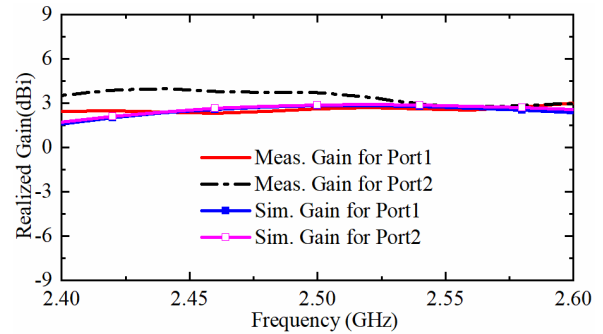


Fig. 8. Simulated and measured realized gain of the two feeding ports of the prototype.

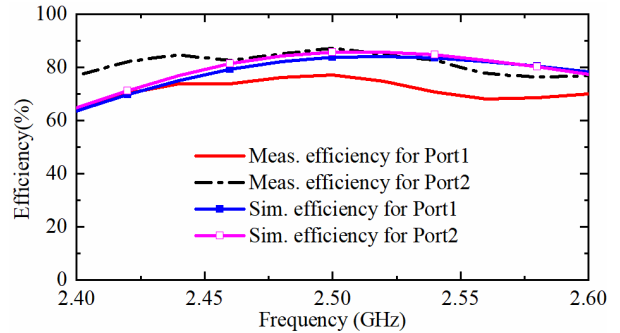


Fig. 9. Simulated and measured radiation efficiency of the two feeding ports of the prototype.

the measurement error, manufacturing discrepancy or fluctuations in the permittivity of the substrate.

The radiation patterns of the two ports were measured, respectively, with the other port matching with a 50  $\Omega$  load. Figs. 8 and 9 present the realized gains and the efficiencies of the proposed antenna. It can be seen from Fig. 8 that the measured realized gains are higher than 2.41 dBi, and the simulated realized gains are over 2.36 dBi. In Fig. 9, the measured radiation efficiencies are above 68%, while the simulated results are higher than 75%. The simulated and measured normalized radiation patterns at 2.5 GHz are presented in Fig. 10. Fig. 10(a) and (b) shows the radiation patterns in E-plane and H-plane for Port1, and Fig. 10(c) and (d) depicts the ones for Port2. The measured and simulated copolarization patterns agree

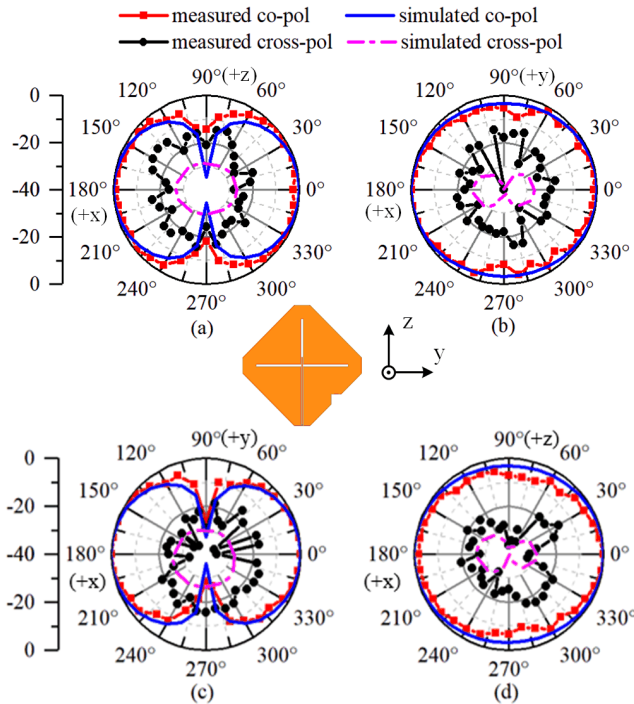


Fig. 10. Simulated and measured normalized radiation pattern of the proposed antenna fed by (a) Port1 in E-plane, (b) Port1 in H-plane, (c) Port2 in E-plane, and (d) Port2 in H-plane at 2.5 GHz.

TABLE II  
COMPARISON BETWEEN THE PROPOSED ANTENNA  
AND PREVIOUS WORKS

Ref	Size( $\lambda^3$ )	BW(GHz)	Isolation	Polarization
[5]	$0.48 \times 0.48 \times 0.016$	2.6-3.9, 40%	30dB	H-pol and V-pol
[14]	$0.65 \times 0.52 \times 0.007$	1.96-2.63, 27.9%	32.6dB	H-pol and V-pol
[17]	$1.00 \times 1.00 \times 0.027$	4.99-6.08 19.7%	30dB	H-pol and V-pol
[18]	$0.85 \times 0.85 \times 0.006$	1.68-2.71, 46.9%	33dB	H-pol and V-pol
[29]	$1.13 \times 1.17 \times 0.037$	5.66-5.91, 4.32%	20dB	$\pm 45$ deg linear
[30]	$0.59 \times 0.59 \times 0.014$	1.68-2.75 23.5%	37dB	$\pm 45$ deg linear
This Work	$0.293 \times 0.293 \times 0.008$	2.44-2.59, 6.0%	30dB	$\pm 45$ deg linear

<sup>a</sup>  $\lambda$  is the wavelength at lowest edge of the radiating band in free space.

with each other well for both Port1 and Port2. The simulated cross-polarization levels are below  $-26$  dB in both E-plane and H-plane compared with the copolarization, and the measured results achieve the cross-polarization levels of lower than  $-20$  dB in the main radiation direction. The total integration of the two patterns is near zero, implying uncorrelation between the two polarizations.

Table II demonstrates the comparison between the proposed antenna and previous dual-polarization antenna designs based on single layer substrate. The items of the comparison include total antenna size, bandwidth, and isolation between two ports. As the table shows, even though the bandwidth of the proposed design is not as wide as the previous designs, the total dimension of the proposed

antenna is much smaller. As we can see, this proposed antenna has an advantage in size.

It needs to be clarified that the proposed design is different from the design in [14], in which the feeding structure and the radiating aperture are apart from each other. Therefore, some area is occupied by the feeding structure. In the proposed antenna, the feeding structure is integrated with the radiating aperture by proper design, without occupying extra area or deteriorating in isolation. And the total dimension is reduced by applying the colocated feeding structure.

#### IV. CONCLUSION

This communication presents a compact dual-polarized antenna based on a single-layer substrate. The colocated feeding structure is applied to compact the total dimensions of the antenna. Two orthogonal polarizations provided by the cross slot are excited by two orthogonal modes in the CPW, respectively. The feeding network is integrated with the dual-polarized cross slot and the ports isolation remains high. Due to the proper design of the feeding structure, high isolation is realized without occupying extra area. Finally, impedance bandwidth of 6% and ports isolation of 30 dB can be achieved with a small size of  $0.293\lambda_0 \times 0.293\lambda_0 \times 0.008\lambda_0$ . The proposed antenna with compact size and simple structure is with potential in space-limited devices for wireless communication applications such as WiFi.

#### REFERENCES

- [1] Z. Bao, Z. Nie, and X. Zong, "A novel broadband dual-polarization antenna utilizing strong mutual coupling," *IEEE Trans. Antennas Propag.*, vol. 62, no. 1, pp. 450–454, Jan. 2014.
- [2] Y. Gou, S. Yang, J. Li, and Z. Nie, "A compact dual-polarized printed dipole antenna with high isolation for wideband base station applications," *IEEE Trans. Antennas Propag.*, vol. 62, no. 8, pp. 4392–4395, Aug. 2014.
- [3] W. C. Zheng, L. Zhang, Q. X. Li, and Y. Leng, "Dual-band dual-polarized compact bowtie antenna array for anti-interference MIMO WLAN," *IEEE Trans. Antennas Propag.*, vol. 62, no. 1, pp. 237–246, Jan. 2014.
- [4] H. Lee and B. Lee, "Compact broadband dual-polarized antenna for indoor MIMO wireless communication systems," *IEEE Trans. Antennas Propag.*, vol. 64, no. 2, pp. 766–770, Feb. 2016.
- [5] D. Lu, L. Wang, E. Yang, and G. Wang, "Design of high-isolation wideband dual-polarized compact MIMO antennas with multiobjective optimization," *IEEE Trans. Antennas Propag.*, vol. 66, no. 3, pp. 1522–1527, Mar. 2018.
- [6] L.-H. Wen *et al.*, "Compact dual-polarized shared-dipole antennas for base station applications," *IEEE Trans. Antennas Propag.*, vol. 66, no. 12, pp. 6826–6834, Dec. 2018.
- [7] D.-L. Wen, D.-Z. Dong, and Q.-X. Chu, "A wideband differentially fed dual-polarized antenna with stable radiation pattern for base stations," *IEEE Trans. Antennas Propag.*, vol. 65, no. 5, pp. 2248–2255, May 2017.
- [8] Y. Gou, S. Yang, Q. Zhu, and Z. Nie, "A compact dual-polarized double E-shaped patch antenna with high isolation," *IEEE Trans. Antennas Propag.*, vol. 61, no. 8, pp. 4349–4353, Aug. 2013.
- [9] C.-X. Mao and Q.-X. Chu, "Compact coradiator UWB-MIMO antenna with dual polarization," *IEEE Trans. Antennas Propag.*, vol. 62, no. 9, pp. 4474–4480, Sep. 2014.
- [10] J. Zhu, S. Li, B. Feng, L. Deng, and S. Yin, "Compact dual-polarized UWB quasi-self-complementary MIMO/diversity antenna with band-rejection capability," *IEEE Antennas Wireless Propag. Lett.*, vol. 15, pp. 905–908, 2016.
- [11] M. S. Khan, A.-D. Capobianco, A. Iftikhar, R. M. Shubair, D. E. Anagnostou, and B. D. Braaten, "Ultra-compact dual-polarized UWB MIMO antenna with meandered feeding lines," *IET Microw., Antennas Propag.*, vol. 11, no. 7, pp. 997–1002, Jun. 2017.
- [12] D. G. Kurup, A. Rydberg, and M. Himdi, "Compact microstrip-T coupled patch antenna for dual polarization and active antenna applications," *Electron. Lett.*, vol. 38, no. 21, pp. 1240–1241, Oct. 2002.
- [13] C.-X. Mao, S. Gao, Y. Wang, F. Qin, and Q.-X. Chu, "Multimode resonator-fed dual-polarized antenna array with enhanced bandwidth and selectivity," *IEEE Trans. Antennas Propag.*, vol. 63, no. 12, pp. 5492–5499, Dec. 2015.

- [14] Y. Li, Z. Zhang, W. Chen, Z. Feng, and M. F. Iskander, "A dual-polarization slot antenna using a compact CPW feeding structure," *IEEE Antennas Wireless Propag. Lett.*, vol. 9, pp. 191–194, 2010.
- [15] Y. Gao, Z. Feng, and L. Zhang, "Compact CPW-fed dielectric resonator antenna with dual polarization," *IEEE Antennas Wireless Propag. Lett.*, vol. 10, pp. 544–547, 2011.
- [16] B. Peng, S. Li, J. Zhu, L. Deng, and Y. Gao, "A compact wideband dual-polarized slot antenna with five resonances," *IEEE Antennas Wireless Propag. Lett.*, vol. 16, pp. 2366–2369, 2017.
- [17] C. H. Lee, S. Y. Chen, and P. Hsu, "Isosceles triangular slot antenna for broadband dual polarization applications," *IEEE Trans. Antennas Propag.*, vol. 57, no. 10, pp. 3347–3351, Oct. 2009.
- [18] X. Jiang, Z. Zhang, Y. Li, and Z. Feng, "A wideband dual-polarized slot antenna," *IEEE Antennas Wireless Propag. Lett.*, vol. 12, pp. 1010–1013, 2013.
- [19] X. Lu, H. Zhang, S. Gu, H. Liu, X. Wang, and W. Lu, "A dual-polarized cross-slot antenna array on a parallel-plate waveguide with compact structure and high efficiency," *IEEE Antennas Wireless Propag. Lett.*, vol. 17, pp. 8–11, Jan. 2018.
- [20] C. Zhou, H. Wong, and L. K. Yeung, "A wideband dual-polarized inductor-end slot antenna with stable beamwidth," *IEEE Antennas Wireless Propag. Lett.*, vol. 17, no. 4, pp. 608–612, Apr. 2018.
- [21] W. Q. Cao, Q. Q. Wang, B. N. Zhang, and W. Hong, "Capacitive probed compact dual-band dual-mode dual-polarisation microstrip antenna with broadened bandwidth," *IET Microw., Antennas, Propag.*, vol. 11, no. 7, pp. 1003–1008, Feb. 2017.
- [22] M. Barba, "A high-isolation, wideband and dual-linear polarization patch antenna," *IEEE Trans. Antennas Propag.*, vol. 56, no. 5, pp. 1472–1476, May 2008.
- [23] B. Li, Y.-Z. Yin, W. Hu, Y. Ding, and Y. Zhao, "Wideband dual-polarized patch antenna with low cross polarization and high isolation," *IEEE Antennas Wireless Propag. Lett.*, vol. 11, pp. 427–430, 2012.
- [24] M. Kaboli, S. A. Mirtaheri, and M. S. Abrishamian, "High-isolation X-polar antenna," *IEEE Antennas Wireless Propag. Lett.*, vol. 9, pp. 401–404, 2010.
- [25] K. L. Wong, H. C. Tung, and T. W. Chiou, "Broadband dual-polarized aperture-coupled patch antennas with modified H-shaped coupling slots," *IEEE Trans. Antennas Propag.*, vol. 50, no. 2, pp. 188–191, Feb. 2002.
- [26] S.-C. Gao, L.-W. Li, M.-S. Leong, and T.-S. Yeo, "Dual-polarized slot-coupled planar antenna with wide bandwidth," *IEEE Trans. Antennas Propag.*, vol. 51, no. 3, pp. 441–448, Mar. 2003.
- [27] Y. Li, Z. Zhang, Z. Feng, and M. F. Iskander, "Dual-mode loop antenna with compact feed for polarization diversity," *IEEE Antennas Wireless Propag. Lett.*, vol. 10, pp. 95–98, 2011.
- [28] X. Wang, W. Chen, Z. Feng, and H. Zhang, "Compact dual-polarized antenna combining printed monopole and half-slot antenna for MIMO applications," in *Proc. IEEE Antennas Propag. Soc. Int. Symp.*, Charleston, SC, USA, Jun. 2009, pp. 1–4.
- [29] O. Yurduseven, D. Smith, and M. Elsdon, "A dual-polarized solar cell stacked microstrip patch antenna with a  $\lambda/4$  DC/RF isolation circuit for 5.8 GHz band WiMAX networks," in *Proc. 8th Eur. Conf. Antennas Propag. (EuCAP)*, Apr. 2014, pp. 1382–1385.
- [30] Z. Zhou, Z. Wei, Z. Tang, and Y. Yin, "Design and analysis of a wideband multiple-microstrip dipole antenna with high isolation," *IEEE Antennas Wireless Propag. Lett.*, vol. 18, pp. 722–726, 2019.